

Human Pulmonary Hyperpolarized ^{129}Xe MRI: a Preliminary Study *

Hao Yang(杨昊)¹, Ke Wang(王科)¹, Hui-Ting Zhang(张会婷)², Jun-Shuai Xie(谢军帅)²,
Guang-Yao Wu(吴光耀)^{1**}, Xin Zhou(周欣)^{2**}

¹The Department of Radiology, Zhongnan Hospital of Wuhan University, Wuhan University, Wuhan 430071

²State Key Laboratory of Magnetic Resonance and Atomic and Molecular Physics, National Center for Magnetic Resonance in Wuhan, Wuhan Institute of Physics and Mathematics, Chinese Academy of Sciences, Wuhan 430071

(Received 29 September 2017)

We study the feasibility and safety of human lung hyperpolarized (HP) ^{129}Xe magnetic resonance imaging (MRI). There is no significant change in physiological parameters before and after the examinations of all subjects. Compared with computed tomography, HP ^{129}Xe MRI is sensitive to earlier and smaller ventilation defects. The distribution of the HP ^{129}Xe MRI signal reflects the pulmonary compliance with the gravity gradient. This is the first application of HP ^{129}Xe MRI ventilation imaging in China, and this technology is expected to provide more useful information for clinical practice.

PACS: 87.80.Lg, 51.60.+a, 28.20.Pr

DOI: 10.1088/0256-307X/35/5/058701

The lung disease situation in China is increasingly severe. Smoking and air pollution are the main risk factors. Inhaled air pollution particles stimulate and cause corrosion of the bronchial and alveolar wall in the lung, leading to a decline in lung function. Therefore, the incidence of lung function-related diseases, such as chronic obstructive pulmonary disease (COPD), asthma, and other respiratory diseases, has increased year by year.^[1]

At present, the evaluation of pulmonary function is mainly dependent on pulmonary function test (PFT) and computed tomography (CT). However, PFT is not sensitive to early changes of emphysema, and also cannot locate the pulmonary emphysema accurately.^[2] Dual-energy CT can find the inhomogeneous distribution of pulmonary blood volume of smoking patients.^[3] Dual-phase (inspiratory and expiratory phase) CT can evaluate the pulmonary function damage area and airway lesions in patients with smoking-related COPD.^[4] Dynamic perfusion CT is sensitive to pulmonary emphysema by calculating the CT value ratio.^[5] However, the presence of ionizing radiation and the use of a large dose of contrast in CT made it unsuitable for patient screening and follow-up observation. Positron emission tomography (PET)-CT and single-photon emission computed tomography (SPECT) are able to obtain functional information, but the image spatial resolution is low and these methods also have the risk of radiation.^[6] The application of proton magnetic resonance imaging (MRI) in the lung is limited, because the image quality is poor due to the low density of protons, low signal-to-noise ratio, and respiratory motion artifacts.

Hyperpolarized (HP) ^{129}Xe MRI overcomes the problems of conventional lung imaging. This imaging method can display the lung structure and function sensitively by using HP ^{129}Xe and ^3He as gas contrast agents. One review has reported the application of HP gas MRI for COPD, asthma, cystic fibrosis, radiation-induced lung injury, and lung transplantation.^[7] Other studies of HP ^{129}Xe MRI in mice and humans have also been proved to be safe, repeatable, and highly sensitive.^[7–10] In this study, we explore the feasibility and safety of human lung HP ^{129}Xe MRI. The characteristics of lung HP ^{129}Xe ventilation imaging were analyzed qualitatively. Physiological parameters such as heart rate, blood pressure, and blood oxygen saturation before and after HP ^{129}Xe MRI were analyzed.

This study was approved by the ethics committee of Zhongnan Hospital of Wuhan University, and all patients signed the informed consent. The study included eight volunteers, three were males and five were females, aged 34–63 y (mean age 53.4 y). All subjects had a complete history of disease and PFT data. Three subjects were diagnosed with pulmonary disease (one of chronic bronchitis, one of asthma, and one smoker), the others were healthy volunteers. The patient with chronic bronchitis was 56 y old and had a history of chronic bronchitis for 10 y. The patient with asthma was 34 y old and had a history of dust allergy and asthma. The smoker was a 52-year-old man and smoked for 30 y, 2 packs per day. All subjects completed pulmonary CT and HP ^{129}Xe MRI scans on the same day. Exclusion criteria included: (1) age <18 or >80 y, (2) lactation or gestation period, (3) history of

*Supported by the National Natural Science Foundation of China under Grant Nos 81227902 and 81625011, the National Key Research and Development Program of China under Grant No 2016YFC1304702, and the Key Research Program of Frontier Sciences of CAS (QYZDY-SSW-SLH018).

**Corresponding author. Email: wuguangy2002@163.com; xinzhou@wipm.ac.cn

© 2018 Chinese Physical Society and IOP Publishing Ltd

arrhythmia, and (4) MRI contraindications.

MRI acquisitions were performed on a 1.5 T MRI scanner (Avanto; Erlangen Siemens, Germany) and a superconducting MRI system for transforming HP ^{129}Xe imaging. The ^{129}Xe gas was hyperpolarized by the homemade rubidium vapor of alkali metal spin-exchange optical pumping system,^[11] which could enhance the sensitivity of HP ^{129}Xe to 60000 times. Before the examination, subjects needed to practice respiratory training twice. They were required to inhale 700 mL of HP ^{129}Xe gas and hold their breath for about 7 s at the end of the expiratory phase during quiet breathing. Heart rate, systolic blood pressure, diastolic blood pressure, and oxygen saturation of the subjects were recorded before and after the examination, and discomfort was also checked. Ventilation imaging used a compressed sensing technique and fast low-angle shot sequence (FLASH). The scanning parameters were as follows: time of echo (TE), 6.75 ms; repetition time (TR), 2.74 ms; matrix, 128×128 ; field of view (FOV), 40×40 ; flip angle (FA), 35° ; pixel, $1.6 \times 1.6 \text{ mm}^2$; layer thickness, 20 mm; layer spacing, 4 mm; layers, 6–8; bandwidth, 250 kHz; and total acquisition time, 6.1–8 s.

Pulmonary CT scanning of all subjects was performed on a dual-energy source 64-slice spiral CT scanner (Somatora Definition; Siemens Erlangen, Ger-

many). The scanning parameters were as follows: voltage, 120 kV; current, 160–180 mAs; matrix, 512×512 ; pitch, 0.75–1.0 mm; and scanning layer thickness, 1 mm. The subjects were placed in a supine position and adopted deep inspiration breath-hold before scanning. The scanning range was from the apex to the bottom of the lung. Multiplanar reconstruction technology was used to observe the lung and bronchi.

Emphysema was the main positive indicator. Two pulmonary radiologists with more than 10 y of experience analyzed the CT and HP ^{129}Xe MRI findings, and they were blind to the medical history and PFT data. Cases were included in the analysis with a consistent diagnosis by them, and disagreements were resolved by consensus. CT images focused on the change in emphysema. The CT diagnostic criteria of emphysema was CT values less than -950 Hounsfield unit (HU). The window center of the observation of emphysema was -975 HU and the window width was 50 HU. MRI focused on the distribution of the whole-lung gas and low-signal defect areas. The *t* test of paired samples was used to examine the changes in vital signs and blood oxygen saturation before and after the examination.

A total of eight subjects (Table 1) were included. All subjects had generally good pulmonary function and had no significant abnormalities.

Table 1. Subject Demographics and PFT. Here BP, blood pressure (mmHg); FEV₁, forced expiratory volume in one second (L); FVC, forced vital capacity (L); and PFT, pulmonary function test.

Subject	Sex	Age(y)	Heart rate	Systolic BP	Diastolic BP	FEV ₁	FVC	FEV ₁ /FVC (%)
1	Female	56	75	128	76	2.29	2.69	85
2	Female	34	90	116	77	2.97	3.67	80
3	Male	52	72	169	106	4.07	4.98	82
4	Female	60	77	110	72	2.23	3.17	70
5	Male	43	84	126	76	3.53	4.36	81
6	Male	63	67	112	68	3.13	4.22	74
7	Female	59	66	103	56	2.33	2.84	82
8	Female	60	67	102	62	2.71	3.66	74

Table 2. Heart rate, systolic blood pressure, diastolic blood pressure, and oxygen saturation of the subjects before and after the examination ($\bar{X} \pm S$). Here BP is blood pressure (mmHg).

	Heart rate	Systolic BP	Diastolic BP	Oxygen saturation
Before examination	74.75±8.68	120.75±21.68	74.13±14.88	97.75±0.71
After examination	74.25±8.03	117.50±14.92	73.88±13.56	97.75±0.89
<i>P</i>	0.516	0.339	0.812	1.000

Except for two subjects who complained of dizziness, the rest of the subjects reported no adverse reaction. The results (Table 2) showed that the heart rate, systolic blood pressure, diastolic blood pressure, and oxygen saturation before and after the examination had no statistically significant changes ($P > 0.05$).

All healthy volunteers showed a homogeneous HP ^{129}Xe MR signal distribution in the lung, while others showed different ventilation defects. As shown in Figs. 1(A)–1(C), the CT images of the chronic bronchitis patient showed emphysema in the left lower lung,

while HP ^{129}Xe MRI displayed not only left lower lung lesion shown on CT, but also some small pulmonary ventilation defects in both lungs. The PFT result of the patient with asthma was normal and the CT images found no obvious abnormalities. However, HP ^{129}Xe MRI showed multiple lung ventilation defects (Figs. 1(D)–1(F)). The lung CT image of the smoker found emphysema in both upper lungs, HP ^{129}Xe MRI showed a wide range of ventilation defect areas larger than CT (Figs. 1(G)–1(I)). The HP ^{129}Xe signal of all eight subjects increased from the front of the lung to

the back of the lung (Figs. 1(J)–1(L)).

HP ^{129}Xe MRI pulmonary ventilation imaging can acquire the structure and function of the lung, and can realize visualization of the lung disease. It reflected the progress of the gas distribution through the trachea and bronchi, and finally into the alveoli after subjects inhaled HP ^{129}Xe gas. In healthy volunteers, the tracheal and bronchi were smooth and the alveolar structure was complete, therefore, ^{129}Xe gas was uniformly distributed in both lungs. Patients with ventilation dysfunction had regional lung structure and function defects due to tracheal spasm, bronchial stenosis, and alveolar damage. HP ^{129}Xe could not enter the damaged bronchi and alveoli, and thus ventilation defect areas in the image could be used to quantitatively evaluate pulmonary ventilation dysfunction. At present, this method has been used in COPD, asthma, cystic fibrosis, radiation-induced lung injury, lung transplantation, and so forth.^[7]

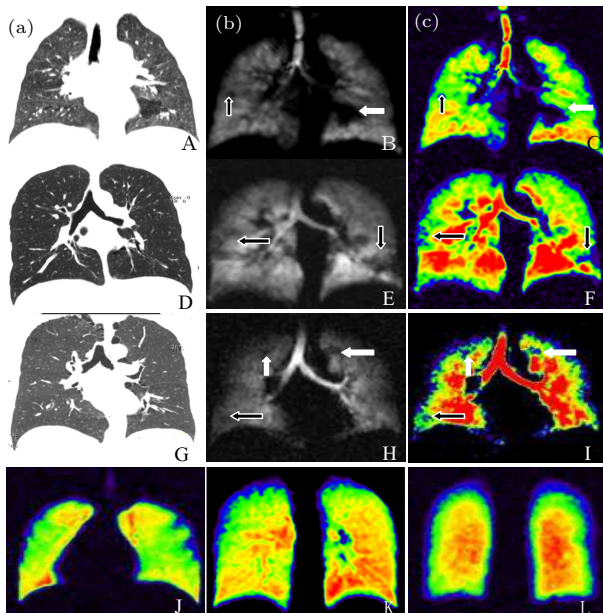


Fig. 1. (A)–(C) CT and HP ^{129}Xe MRI of a 56-year-old woman with a history of chronic bronchitis. CT only showed density reduction area (white arrow) in the left lower lung, and HP ^{129}Xe MRI showed the left lower lung lesion (white arrow) and more small-ventilation-defect area (black arrow). (D)–(F) CT and HP ^{129}Xe MRI of a 34-year-old woman with a history of asthma. CT showed no significant abnormalities, while HP ^{129}Xe MRI showed multiple ventilation defect areas (black arrow) in both lungs. (G)–(I) CT and HP ^{129}Xe MRI of a 52-year-old male smoker who smoked for more than 10 y. CT showed emphysema areas (white arrow) in both upper lungs. In addition to the upper lung ventilation defects (white arrow), HP ^{129}Xe MRI displayed more extensive ventilation defect areas (black arrow). (J)–(L) The coronal HP ^{129}Xe MRI of a single healthy subject at different slices. In the direction of gravity, the coronal image signal intensity increased from the front to the back of the lung.

HP ^{129}Xe pulmonary ventilation MRI is a nonradiation-based system and sensitive to lung venti-

lation defects. ^{129}Xe is an inert and nontoxic gas contrast agent. Clinical research has confirmed its safety in human MRI.^[9] In the present study, eight subjects successfully completed the examination. Except for two patients complaining of dizziness, the remaining subjects had no adverse reactions. The vital signs and blood oxygen saturation before and after the examination found no significant changes ($P > 0.05$), which was consistent with other reports.^[7] HP ^{129}Xe gas can acquire high signal enhancement, and the image signal-to-noise ratio in this study could reach the diagnostic requirement and clearly display the ventilation defects.

HP ^{129}Xe MRI pulmonary gas signal distribution may respond to lung compliance with the gravity gradient. In this study, eight subjects were scanned in the supine position. In the direction of gravity, HP ^{129}Xe MRI signal distribution of all subjects presented a gradient-like increasing trend from the anterior to the posterior lung, indicating that HP ^{129}Xe distribution might be under the effect of gravity. In the non-gravity-dependent direction (left and right directions), no obvious difference in MRI signal was observed between the left and right lungs in the same coronal image. Research^[12] had confirmed the gravity gradient distribution of pulmonary blood perfusion, but study on the distribution of pulmonary gas is still lacking. This study found lung compliance of gravity gradient characteristics, and the reason might be that in the non-gravity-dependent direction, the HP ^{129}Xe molecule in the alveoli was mainly carrying out an irregular Brown motion. Therefore, a uniform distribution was present in the same coronal plane of the left and right lungs. On one hand, as the ^{129}Xe molecule density (5.9 g/L) was higher than air density (1.3 g/L), more ^{129}Xe gas molecules were distributed in the dorsal lung. On the other hand, due to the physiological characteristics of the lung itself, the upper lung's intrathoracic pressure was lower than that of the lower lung under gravity, which decreased the upper alveolar compliance and gas flow.

COPD was characterized by an irreversible airway obstruction and alveolar destruction. It had two pathological processes, chronic bronchitis and pulmonary emphysema. Although the PFT result of the chronic bronchitis case in this study did not meet the diagnostic criteria of COPD, HP ^{129}Xe MRI presented ventilation defect areas, suggesting that the patient had early COPD and HP ^{129}Xe MRI could find emphysema earlier than CT. Kirby *et al.*^[7] measured ventilation defect percentages (VDPs) in patients with COPD using ^3He and ^{129}Xe MRI, and the results showed that VDPs were related to forced expiratory volume in one second (FEV_1), $\text{FEV}_1/\text{forced vital capacity (FVC)}$, diffusing capacity of carbon monoxide (DLCO), and other pulmonary function parameters.

Kaushik *et al.*^[13] found that HP ¹²⁹Xe MRI could show lesions that CT failed to find, and these lesions might be early mild inflammatory areas and a potential therapeutic target. These findings suggested that HP ¹²⁹Xe MRI was highly sensitive to the early diagnosis of COPD. Asthma is a chronic airway inflammatory disease characterized by reversible airflow limitation with dyspnea, cough, chest distress, and wheezing. Traditional PFT could only reflect the whole-lung airflow limitation and was not sensitive to the small airway lesions. The diagnostic value of radionuclide imaging, PET, x-ray, and CT in asthma was limited. The HP ¹²⁹Xe MRI study of patients with asthma^[14] showed that HP ¹²⁹Xe MRI signal distribution in the lung was not homogeneous and had obvious ventilation defect regions that CT failed to show. These regions enlarged and increased after activities or choline load and disappeared after bronchodilator agent treatment, and the lung function of the subjects improved after administration. Qing *et al.*^[15] found that the alveolar septal wall thickened in patients with asthma and the whole-lung signal was heterogeneous. In this study, the PFT and CT of the patient with asthma had no obvious abnormality, whereas the HP ¹²⁹Xe MRI showed ventilation defects in both lungs, which might reflect the existence of small airway inflammatory remodeling and local ventilation dysfunction. Although PFT did not find significant abnormality in the long-term smoker in this study, emphysema areas were found in both lungs. Smoking can lead to the destruction of the structure and dysfunction of pulmonary vascular endothelial cells. Long-term smoking can also lead to alveolar damage and emphysema, resulting in decreased pulmonary perfusion and ventilation dysfunction. The dynamic contrast-enhanced (DCE)-MRI study^[16] found decreased lung function in smokers. Various degrees of emphysema were found on CT, and DCE-MRI displayed a perfusion defect on the corresponding areas. Smokers may have similar emphysema changes as COPD. In the study by Kaushik *et al.*,^[13] patients with severe COPD were always high-risk smokers, and HP ¹²⁹Xe MRI showed obvious heterogeneous changes associated with multiple ventilation defect areas. This was consistent with our study, suggesting that HP ¹²⁹Xe MRI could be used to screen for early COPD in high-risk smokers.

One of the limitations of this study is that the sample size was small. We obtained the preliminary result of human pulmonary HP ¹²⁹Xe MRI. A large-sample clinical study is required to further validate the findings. This study for the first time accomplished HP ¹²⁹Xe MRI ventilation imaging in China. This imaging method could safely and effectively evaluate lung ventilation defects and sensitively display early stage lesions that were not visible on CT; the lung compliance with the gravity gradient was also presented.

The authors declared no conflicts of interest.

References

- [1] Hu G, Zhong N and Ran P 2015 *J. Thorac Dis.* **7** 59
- [2] Matin T N, Rahman N, Nickol A H, Chen M, Xu X, Stewart N J, Doel T, Grau V, Wild J M and Gleeson F V 2017 *Radiology* **282** 857
- [3] Iyer K S, Newell J J, Jin D, Fuld M K, Saha P K, Hansdotir S and Hoffman E A 2016 *Am. J. Respir. Crit. Care Med.* **193** 652
- [4] Koyama H, Ohno Y, Fujisawa Y, Seki S, Negi N, Murakami T, Yoshikawa T, Sugihara N, Nishimura Y and Sugimura K 2016 *Eur. J. Radiol.* **85** 352
- [5] Guan Y, Xia Y, Fan L, Liu S Y, Yu H, Li B, Zhao L M and Li B 2015 *Acta Radiol.* **56** 573
- [6] Saruya S, Yamashiro T, Matsuoka S, Matsushita S, Yagihashi K and Nakajima Y 2017 *Lung.* **195** 179
- [7] Kirby M, Svenningsen S, Owrangi A, Wheatley A, Farag A, Ouriadov A, Santyr G E, Etemad-Rezai R, Coxson H O, McCormack D G and Parraga G 2012 *Radiology* **265** 600
- [8] Mugler J R and Altes T A 2013 *J. Magn. Reson. Imaging.* **37** 313
- [9] Driehuys B, Martinez-Jimenez S, Cleveland I, Metz G M, Beaver D M, Nouns J C, Kaushik S S, Firszt R, Willis C, Kelly K T, Wolber J, Kraft M and McAdams H P 2012 *Radiology* **262** 279
- [10] Li H, Zhang Z, Zhao X, Sun X, Ye C and Zhou X 2016 *Magn. Reson. Med.* **76** 408
- [11] Zhou X 2011 *In vivo NMR Imaging: Methods and Protocols* (New York: Humana Press) pp 189–204
- [12] Ax M, Sanchez-Crespo A, Lindahl S, Mure M and Petersson J 2017 *J. Appl. Physiol.* **122** 1445
- [13] Kaushik S S, Robertson S H, Freeman M S, He M, Kelly K T, Roos J E, Rackley C R, Foster W M, McAdams H P and Driehuys B 2016 *Magn. Reson. Med.* **75** 1434
- [14] Svenningsen S, Kirby M, Starr D, Leary D, Wheatley A, Maksym G N, McCormack D G and Parraga G 2013 *J. Magn. Reson. Imaging.* **38** 1521
- [15] Qing K, Mugler J R, Altes T A, Jiang Y, Mata J F, Miller G W, Ruset I C, Hersman F W and Ruppert K 2014 *NMR Biomed.* **27** 1490
- [16] Xia Y, Guan Y, Fan L, Liu S Y, Yu H, Zhao L M and Li B 2014 *COPD.* **11** 510